

# Monitoring of Morphological Change in Lam Phachi River Using Geo-informatics System



Thanat Saprathet, Chudech Losiri, Asamaporn Sitthi,  
and Jeerapong Laonamsai 

**Abstract** Nowadays, economic and industrial development along the Lam Phachi River in Ratchaburi and Kanchanaburi provinces is accelerating and increasing water demand. Therefore, weirs were built to preserve the water demand, and the sand extraction businesses were also carried out to support economic expansion. These activities resulted in river morphological change relative to the past. Additionally, climate change has resulted in a rapid change in river discharge and riverbank erosion each season. To monitor the morphology of the river, normalized difference water index (NDWI), soil adjusted vegetation index (SAVI), and a maximum likelihood classification were used to analyze the pattern using remotely sensed images obtained from the Thaichote satellite between 2013 and 2015 and the Sentinel-2A satellite between 2017 and 2019. The results indicated that the Lam Phachi River follows a dendritic drainage pattern, with similar characteristics of riverbank erosion in all directions. The rivers obtained from the NDWI extraction had an accuracy of 94.11% and an analytical precision of 95.15%. The SAVI results indicated an accuracy of 93.17% and a precision of 94.33%. The maximum likelihood classification results showed an accuracy of 96.67% and an analytical precision of 97.47%. The stream extraction method based on the maximum likelihood classification is the most accurate. It was found that the erosion was a lot in the middle of the river, and most of the deposition areas are found at the end of the river. However, the NDWI and SAVI extractions are less accurate in this study area due to water hyacinth and a slight difference in water content between the riverbank and the water bodies.

---

T. Saprathet · C. Losiri (✉) · A. Sitthi  
Department of Geography, Faculty of Social Sciences, Srinakharinwirot University,  
Bangkok, Thailand  
e-mail: [chudech@g.swu.ac.th](mailto:chudech@g.swu.ac.th); [asamaporn@g.swu.ac.th](mailto:asamaporn@g.swu.ac.th)

J. Laonamsai  
Department of Civil Engineering, Faculty of Engineering, Naresuan University,  
Phitsanulok, Thailand

© The Author(s), under exclusive license to Springer Nature  
Switzerland AG 2023

W. Boonpook et al. (eds.), *Applied Geography and Geoinformatics for Sustainable Development*, Springer Geography,  
[https://doi.org/10.1007/978-3-031-16217-6\\_4](https://doi.org/10.1007/978-3-031-16217-6_4)

**Keywords** Remote sensing · SAVI · NDWI · Maximum likelihood classification · Riverbank erosion · River morphology

## 1 Introduction

Water is a vital resource on the planet that all organisms require to survive. It is a significant world component, accounting for up to three-fourths of its surface. Although water is abundant, population growth and economic expansion have increased the water demand. Due to environmental and climatic changes, natural disasters such as floods, droughts, landslides, and soil erosion are becoming more frequent and severe [1]. Additionally, industrial expansion contributes to the escalating water pollution problem in the modern era [2].

Thailand has encountered water resource issues on various dimensions, including water quality, drought, flooding, and riverbank erosion [3]. Riverbank erosion is primarily caused by river curvature, discharge, near-surface wind speed, and waves [4]. Floods affect geographical change, such as riverbank erosion, because the force of the river flow exceeds the riverbank's resistance capacity. In addition, human-caused bank erosion occurs because of transportation and the sand mining industry [5]. The Lam Phachi River originates in the Tenasserim Mountains in western Thailand. Because of its curvature and geological setting, the Lam Phachi River has been eroded [6]. As a result, the water consumed by humans is muddy and sedimentary, posing health risks and affecting agricultural products. Sand vacuuming also results in the collapse of riverbanks and alters the flow of the river [7].

The issues mentioned above in the Lam Phachi River are critical. They must be resolved immediately, and they may have a long-term impact on natural resources and humans, including the livelihoods and utilities of people living along the river. The remote sensing method has been widely used to monitor the eroded and deposited areas of the river [8, 9]. Thus, the current study used remote sensing to investigate river morphology and riverbank erosion and deposition in the Lam Phachi River. Thaichote and Sentinel-2A satellite images were used in this study. Three methods including the soil adjusted vegetation index (SAVI), the normalized difference water index (NDWI), and the maximum likelihood image classification were used to extract the river morphological change. This study will contribute valuable information about river morphology and bank erosion to the relevant government organization to develop sustainable river management policies.

## 2 Study Area

The Lam Pachi River basin is located in Ratchaburi and Kanchanaburi provinces and covers an area of 2550 km<sup>2</sup>. The Lam Pachi River flows through Ratchaburi Province from its source in the Tenasserim Hills. In Kanchanaburi Province, the

river merges with the Mae Klong River. The majority of the Lam Phachi basin is located in Ratchaburi, while a small portion is located in Kanchanaburi. The main channel measures 130 km in length. The river runoff flows from the south to the north. Stream flow is seasonal in nature, with two distinct seasons: wet and dry. October has the highest discharge, averaging 56 m<sup>3</sup>/s, while January through March has the lowest, averaging less than 3 m<sup>3</sup>/s [10]. Additionally, the most significant environmental problems are related to river flow during the two previous seasons: flooding during the wet season and drought during the dry season (Fig. 1).

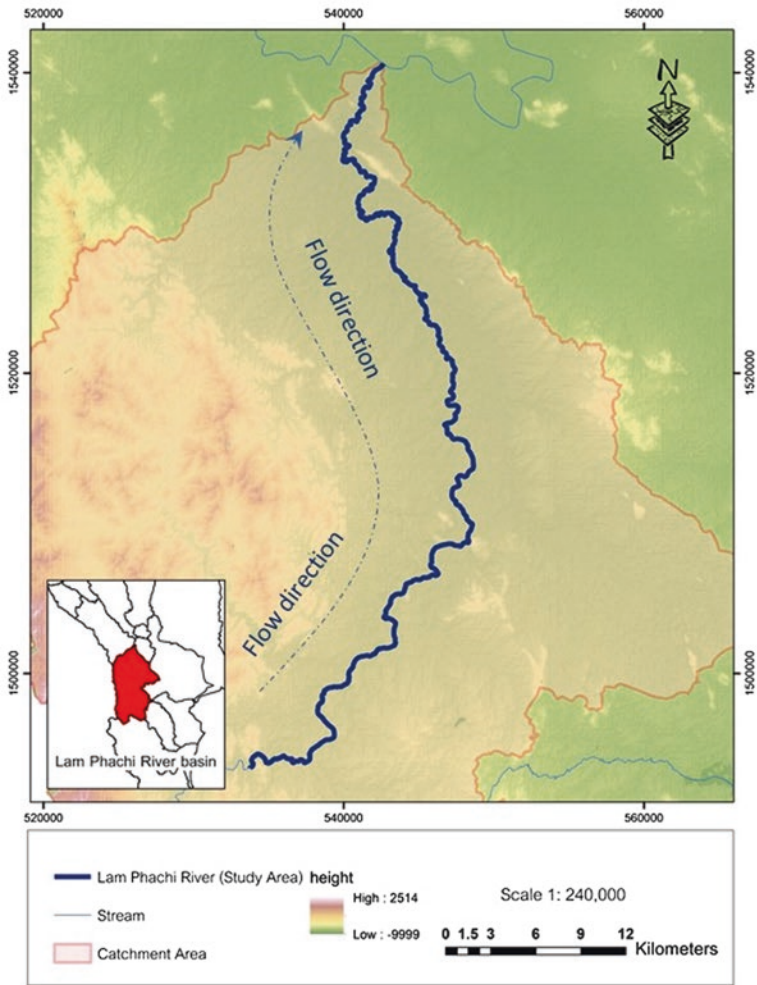


Fig. 1 The study area in the Lam Phachi River basin

### 3 Data and Method

#### 3.1 Satellite Images

##### 3.1.1 Thaichote Satellite

Thaichote, as known as THEOS, was wholly owned and operated by the Thai Ministry of Science and Technology's Space Agency (GISTDA). It provided Thailand with globally georeferenced image products and image processing capabilities for use in cartography, land use, agricultural monitoring, forestry management, coastal zone monitoring, and flood risk management [11]. It was intended to be a small satellite weighing 750 kg. It was launched into low earth orbit in 2008, reaching an altitude of 822 km with a 98-degree inclination [12]. It is equipped with optical imagery capable of detecting objects in the visible to near-infrared range. The image resolution is 15 m perpendicular to the earth's surface, with a width of 90 km. The Thaichote satellite images are smaller than the study area. Three images were mosaiced using the Geographic Information System (ArcMap) program to ensure the data's completeness and continuity.

##### 3.1.2 Sentinel-2A

Sentinel-2A is a European optical imaging satellite launched in 2015 at the height of 786 km as part of the Copernicus Programme of the European Space Agency [13]. The satellite is equipped with a wide-swath, high-resolution multispectral imager with a resolution of 10–60 m and 13 spectral bands [14]. It conducts global-terrestrial observations to support services such as forest monitoring, detection of land cover changes, and natural disaster management. Table 1 details the satellite images used for Thaichote and Sentinel-2A.

**Table 1** Details of satellite images used in this study

Satellite	Date	Month	Year	Path/ row	Source
Thaichote	4	February	2013	150/35	GISTDA
	28	February	2015		
Sentinel-2A	20	January	2017	R104	USGS
	26	November	2019		

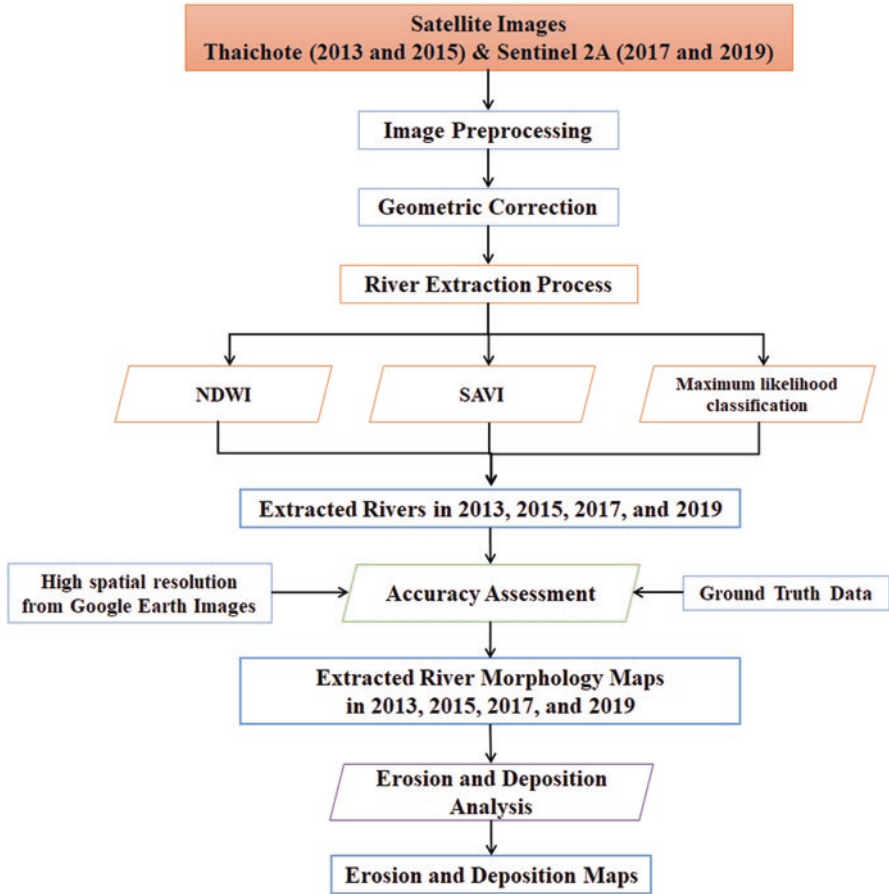


Fig. 2 The flowchart of methodology for the Lam Phachi River extraction

### 3.2 River Extraction Method

To extract the Lam Phachi River from the satellite images, this study designed the overall methodology as shown in Fig. 2. After downloading the satellite image from the online data archives, all images were passed into data preprocessing processes such as atmospheric correction, geometric correction, and image mosaicking. Then, all images were also resampled to 15-meter spatial resolution.

To analyze satellite images, three different methods were used to extract streamlines: the soil adjusted vegetation index (SAVI), the normalized difference water index (NDWI), and the maximum likelihood image classification method. The streamlines from all three methods were combined to create a riverbank line that is complete and accurate, with more efficient and precise data for the analysis.

### 3.2.1 Normalized Difference Water Index (NDWI)

The normalized difference water index (NDWI) is used to highlight open water features in satellite images by utilizing the NIR (near-infrared) and GREEN (visible green) spectral bands [15]. The index is given as:

$$NDWI = (GREEN - NIR) / (GREEN + NIR) \tag{1}$$

NDWI is an appropriate vegetation index for distinguishing land from water. This is because the surface of the water has a high absorption of electromagnetic radiation and low radiation reflectance. There is, however, an error in estimating the construction site as water. As a result, it is crucial to determine the ratio of NIR and GREEN wavelengths. The NDWI value is between  $-1$  and  $1$ , with  $1$  indicating the presence of water bodies or extremely high humidity and  $-1$  indicating a dry area or no moisture [16]. The NDWI was calculated for this study using the raster calculator toolbox in the ArcMap program. The NDWI value between  $0.19$  and  $0.58$  indicates the presence of a water body, as illustrated in Fig. 3a.

### 3.2.2 Soil Adjusted Vegetation Index (SAVI)

NDWI products derived empirically are inherently unstable, varying with soil color, soil moisture, and saturation effects caused by dense vegetation [17]. As a result, the SAVI was created to account for the differential extinction of red and near-infrared light within the vegetation canopy. The index is a transformation technique that reduces the influence of spectral vegetation indices that use red (RED) and near-infrared (NIR) wavelengths on soil brightness [18]. The SAVI index is given as:

$$SAVI = ((NIR - RED) / (NIR + RED + L)) \times (1 + L) \tag{2}$$

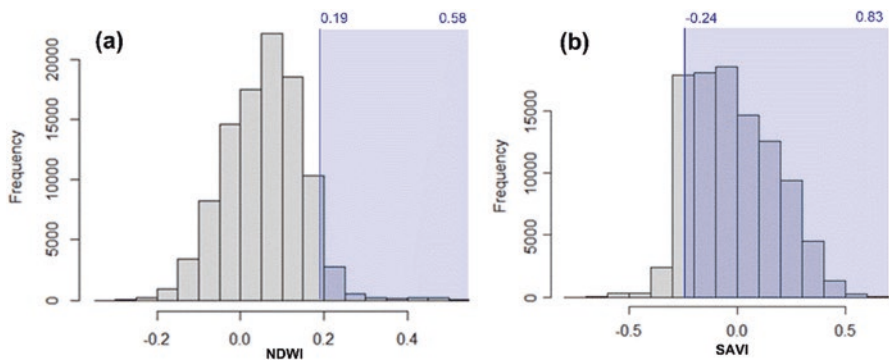


Fig. 3 Histogram of (a) NDWI value and (b) SAVI value

where  $L$  is a factor for adjusting the canopy background. The  $L$  value of 0.5 was discovered in reflectance space to minimize soil brightness variations and eliminate the need for additional calibration for different soils [19]. It was found that the transformation virtually eliminates soil-induced variations in vegetation indices. The study extracts satellite imagery data with SAVI using the red and near-infrared bands via a raster calculator in the ArcMap program. The SAVI values ranged from  $-0.24$  to  $0.83$  (Fig. 3b).

### 3.2.3 Image Classification Method

The training area was defined using supervised classification and shapefiles to visualize the river line. The maximum likelihood classifier was used to extract the water body, which classifies the data by considering each data type's mean and covariance matrix [20]. For this study, satellite image data, including visible and near-infrared wavelengths, were extracted via classification of image data using ArcMap's functional classification [21]. It begins by selecting a representative sample of the training sites, which are the water areas. It is assumed that each data type has a normal distribution and then determines which data type has the highest probability of containing each image point.

## 3.3 Data Validation

A confusion matrix summarizes prediction results on image classification [22]. Correct and incorrect predictions are outlined and broken down by class using count values. Next, this study compared the observed classification set to the predicted classification set. Four distinct outcomes are possible in any given column [23, 24], as illustrated in Table 2. Firstly, the classifier correctly identified the water sample. This is referred to as a true positive (TP). Secondly, the classifier incorrectly classifies the water sample as land or vegetation, resulting in a false-negative (FN) result. Thirdly, the classifier misclassifies the land sample as water. This condition is referred to as a false-positive result (FP). Fourthly, the classifier correctly identifies the land sample as a true negative result (TN).

By overlaying the riverbanks from the Google Earth base map on the river line data extracted from satellite imagery, this study validates the river line data extracted from satellite imagery. To begin, actual points were chosen to compare streamline

**Table 2** Confusion matrix

Predicted/actual	Yes	No
Yes	TP	FP
No	FN	TN

classifications for each method applied to the area. Finally, the result was incorporated into the confusion matrix, as shown in Table 2. The following accuracy and precision values were calculated:

$$\text{Accuracy} = (TP + TN) / (TP + TN + FP + FN) \quad (3)$$

$$\text{Precision} = TP / (TP + FP) \quad (4)$$

## 4 Results and Discussion

### 4.1 Streamline Extraction

Figure 4 shows the streamlines extracted from Thaichote and Sentinel-2A satellite images in 2013, 2015, 2017, and 2019 using the NDWI, SAVI, and image classification. The result indicates that for each year of interest, the streamlines extracted using these three methods are not significantly different (Fig. 4).

To validate the results, the 100 sample points of the Lam Phachi riverbank from the high-resolution images of the Google Earth [25] and a ground survey were utilized and summarized in a confusion matrix, including checks for accuracy and precision (Table 3). According to the confusion matrix, the streamline obtained from the NDWI extraction was 95% accurate and 97% precise. The river obtained through the SAVI extraction was 91% accurate and 93% precise. The streamline extracted via image classification produced the most accurate result. According to Table 3, the accuracy is 97%, and the precision is 98%. It was followed by the NDWI and SAVI extraction results.

### 4.2 River Morphology

The Lam Phachi River flows from south to north (Fig. 1). The morphology of the upstream river is dominated by rock, has a steep slope, and results in a relatively narrow V-shaped valley [26]. Additionally, weirs were constructed, giving the river the appearance of a meander downstream of the weir. The area between the mid-stream and downstream is flat. As a result, the riverbank was eroded, and the convex bank was deposited. The depositional bank was formed by accumulating coarse sand sediment and gravel. This mechanism alternates the ridge with a swale, referred to as a sand shoal, developing the Lam Phachi River's waterways. The streams form a network defined as the dendritic drainage pattern [27]. Dendritic drainage patterns are prevalent in rocky terrain. The riverbank erosion characteristics are similar in all directions. As a result, an overlay technique was used each year to obtain representative river lines (Fig. 5).



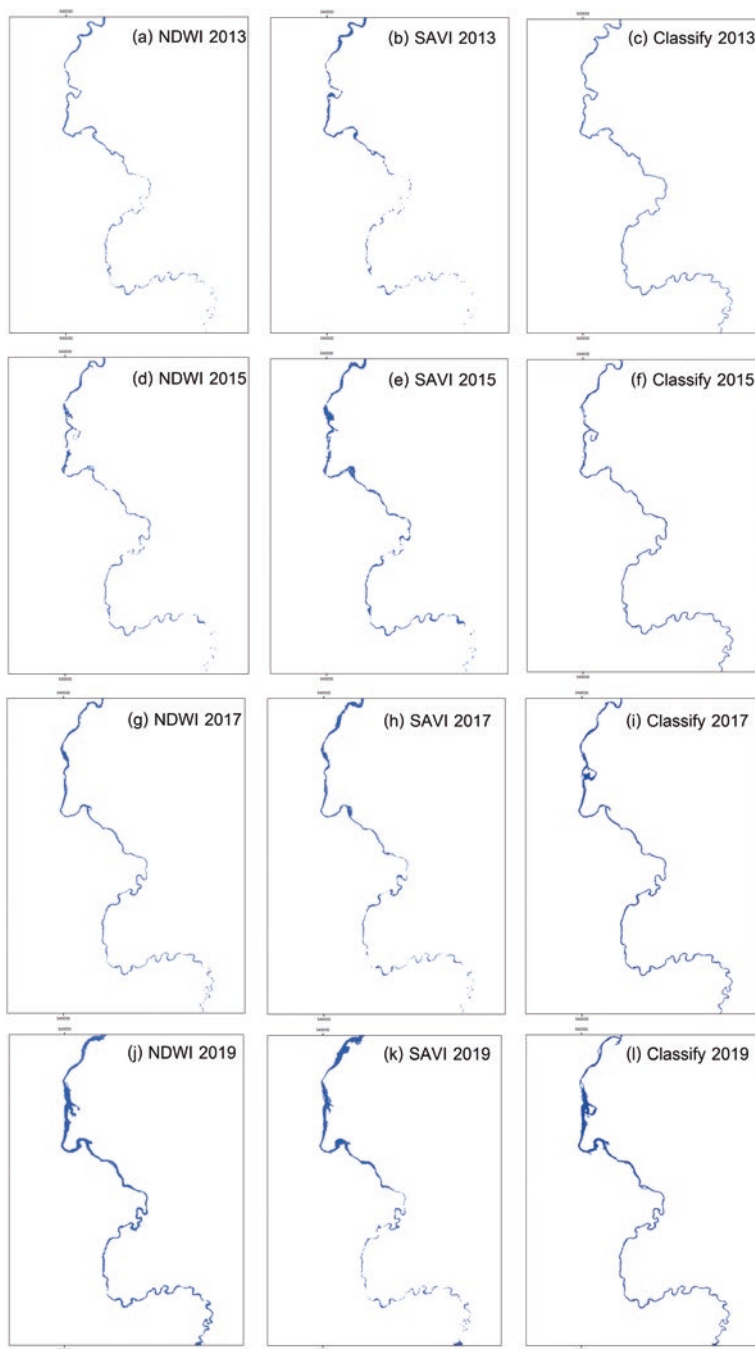


**Fig. 4** Extracted streamlines using NDWI, SAVI, and the maximum likelihood classification

**Table 3** Confusion matrix of the results from NDWI, SAVI, and image classification

Method	Actual Prediction	Water	Others	Accuracy (%)	Precision (%)
NDWI	Water	81	3	95	97
	Others	2	14		
SAVI	Water	90	3	91	93
	Others	6	1		
Maximum likelihood classification	Water	92	2	97	98
	Others	1	5		

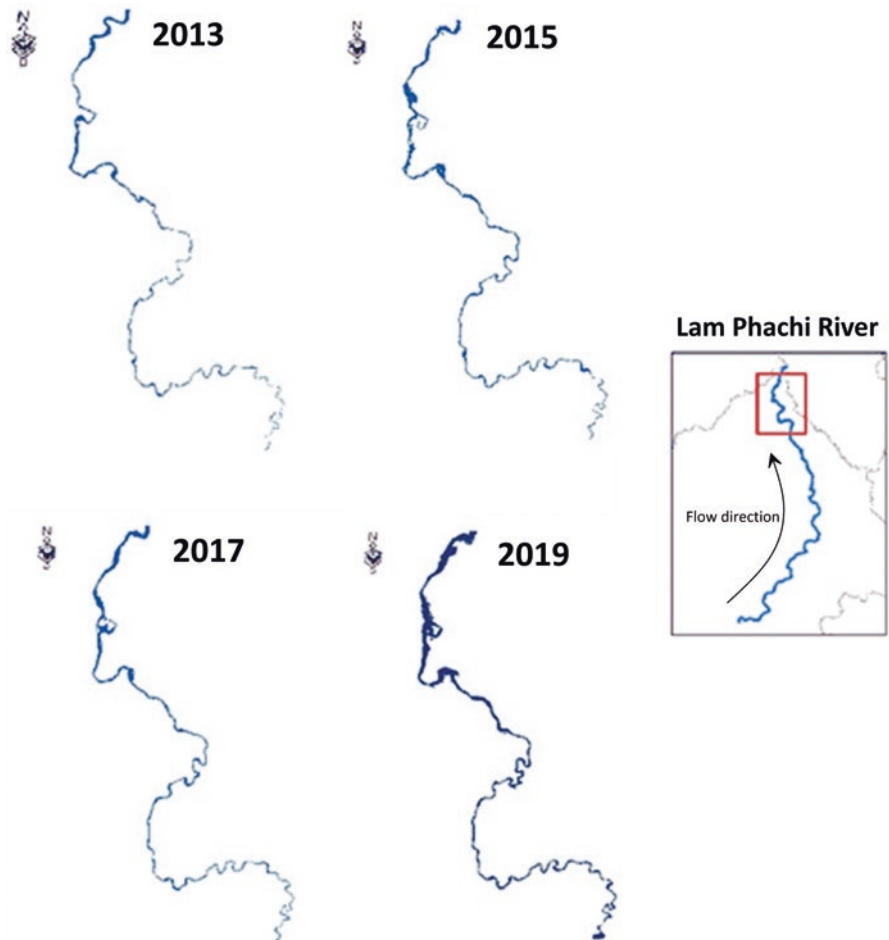


**Fig. 5** An overlaid streamline between NDWI, SAVI, and maximum likelihood classification methods during (a) 2013, (b) 2015, (c) 2017, (d) 2019

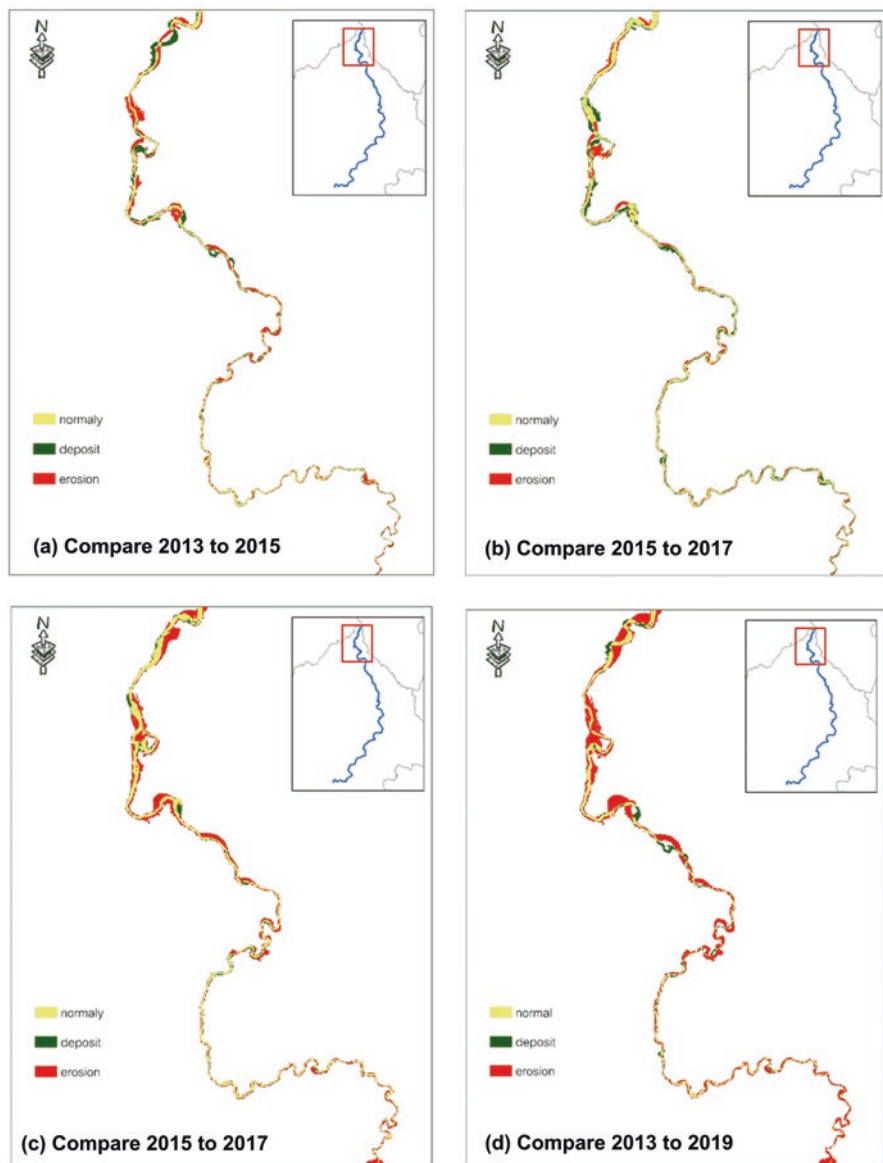


**Fig. 6** Riverbank erosion and deposition along the Lam Phachi river between (a) 2013 and 2015, (b) 2015 and 2017, (c) 2017 and 2019, and (d) 2013 and 2019

### 4.3 Riverbank Erosion and Deposition

This study used the overlay technique to analyze changes in river morphology. Streamlines were overlaid and combined from three different methods (the maximum likelihood classification, NDWI, and SAVI) to represent the better quality of the river morphology in 2013, 2015, 2017, and 2019. Each period was examined for changes in river morphology. Figure 6a depicts riverbank erosion and deposition from 2013 to 2015. By overlapping the data for eroded (red) and deposited (green) areas along the Lam Phachi River, it is possible to calculate that the eroded area equals 0.89 km<sup>2</sup> and the deposition area equals 1.11 km<sup>2</sup>. Considering the changes in river morphology between 2015 and 2017, the result indicates that the erosional area is 0.91 km<sup>2</sup> and there are 0.85 km<sup>2</sup> of depositional area (Fig. 6b).

Additionally, the streamlines between 2017 and 2019 were overlaid (Fig. 6c). The erosional area is estimated to be 1.52 km<sup>2</sup>. The depositional area is approximately 0.34 km<sup>2</sup> in size. Compared to the previous period of 2013–2017, the erosion is more pronounced due to dam operation. Additionally, erosion and deposition along the Lam Phachi River were considered for the entire period of 2013–2019 (Fig. 6d). Erosion had a greater impact than deposition. Erosion totaled 1.87 km<sup>2</sup>. The area affected by the deposition is 0.67 km<sup>2</sup>. These findings confirm that landlords have been losing their fields at an alarming rate [7].

## 5 Conclusion

This study uses the NDWI, the SAVI, and the maximum likelihood classification to reflect progress in the river morphology in Lam Phachi River between 2013 and 2019 using Sentinel 2-A and Thaichote satellites. The extracted streamline results indicated that the maximum likelihood classification method yielded the most accurate with a 97% accuracy and 98% precision. Additionally, the streamline from that method contained the complete characteristics of the river. On the other hand, the SAVI and NDWI produced less accurate results because some sections of the river line were missing, particularly those with narrow channels. Therefore, the Lam Phachi River's stream patterns are described as dendritic, with similar erosion characteristics along the riverbank in all directions.

The erosion and deposition of the Lam Phachi River were analyzed from the extracted streamlines. The erosion and deposition could be found along the river. Between 2013 and 2019, an area of 1.88 km<sup>2</sup> was eroded. The most eroded zones were in the middle and downstream of the river, where a sand mining industry and dam operation existed. As a result, the river curved back and forth across the landscape as it flowed over gently sloping terrain. It made the river meandering. In comparison, between 2013 and 2019, the landfill area was 0.67 km<sup>2</sup>. It was because the river discharge was low and the watercourse has changed direction, the most of the deposited land was in the middle of the Lam Phachi River.

## References

1. Ahuja, S.: Lessons learned from water disasters of the world, in *Separation Science and Technology*, pp. 417–427. Elsevier (2019)
2. Pashtoon, R., Zaki, Z., Haqbin, N.: Empirical study on international tourism and economic growth of Thailand: An ARDL-ECM bounds testing approach. *J. Enterp. Dev.* **4**(1), 28–48 (2022)
3. Laonamsai, J., Ichianagi, K., Patsinghasanee, S.: Isotopic temporal and spatial variations of tropical rivers in Thailand reflect monsoon precipitation signals. *Hydrol. Process.* **35**(3), e14068 (2021)
4. Grove, R., Croke, J., Thompson, C.: Quantifying different riverbank erosion processes during an extreme flood event. *Earth Surf. Process. Landf.* **38**(12), 1393–1406 (2013)
5. Lusiagustin, V., Kusratmoko, E.: Impact of sand mining activities on the environmental condition of the Komerang river, South Sumatera. 2017. AIP Publishing LLC (2017)
6. ThaiPBS, Sand mining activity in the Lam Phachi River, <https://news.thaipbs.or.th/content/282181>. Last accessed 29 May 2019.
7. MGROnline, Ratchaburi residents complained that sand mining business cause riverbank erosion, <https://mgronline.com/local/detail/9610000097297>. Last accessed 29 May 2019.
8. Aher, S.P., Bairagi, S.I., Deshmukh, P.P., Gaikwad, R.D.: River change detection and bank erosion identification using topographical and remote sensing data. *Int J Appl Inf Syst.* **2**(3), 1–7 (2012)
9. Kumm, M., Lu, X., Rasphone, A., Sarkkula, J., Koponen, J.: Riverbank changes along the Mekong River: Remote sensing detection in the Vientiane–Nong Khai area. *Quat. Int.* **186**(1), 100–112 (2008)
10. Areerachakul, S., Junsawang, P.: Rainfall-Runoff relationship for streamflow discharge forecasting by ANN modelling. 2014. IEEE (2014)
11. Tanarat, S., Popattanachai, P., Kasetkasem, T.: THAICHOTE level 1A production using SIPRO procedure. In: 2016 13th International Conference on Electrical Engineering/Electronics, Computer, Telecommunications and Information Technology (ECTI-CON) 2016. IEEE (2016)
12. Vongsantivanich, W., R. Sachasiri, P. Navakitkanok, J. Plaidoung, D. Niammuad, P. Popattanachai. The Evolution of GISTDA Satellite Control Center. 2014
13. Gascon, F., C. Bouzinac, O. Thépaut, M. Jung, B. Francesconi, J. Louis, V. Lonjou, B. Lafrance, S. Massera, A. Gaudel-Vacaresse, Copernicus Sentinel-2A calibration and products validation status. *Remote Sens. (Basel)* **9**(6), p. 584 (2017).
14. Li, J., Roy, D.P.: A global analysis of Sentinel-2A, Sentinel-2B and Landsat-8 data revisit intervals and implications for terrestrial monitoring. *Remote Sens. (Basel)*. **9**(9), 902 (2017)
15. Gao, B.-C.: NDWI—A normalized difference water index for remote sensing of vegetation liquid water from space. *Remote Sens. Environ.* **58**(3), 257–266 (1996)
16. McFeeters, S.K.: The use of the Normalized Difference Water Index (NDWI) in the delineation of open water features. *Int. J. Remote Sens.* **17**(7), 1425–1432 (1996)
17. da Silva, V.S., Salami, G., da Silva, M.I.O., Silva, E.A., Monteiro Junior, J.J., Alba, E.: Methodological evaluation of vegetation indexes in land use and land cover (LULC) classification. *Geol. Ecol. Landscape.* **4**(2), 159–169 (2020)
18. Huete, A.R.: A soil-adjusted vegetation index (SAVI). *Remote Sens. Environ.* **25**(3), 295–309 (1988)
19. Qi, J., Chehbouni, A., Huete, A.R., Kerr, Y.H., Sorooshian, S.: A modified soil adjusted vegetation index. *Remote Sens. Environ.* **48**(2), 119–126 (1994)
20. Strahler, A.H.: The use of prior probabilities in maximum likelihood classification of remotely sensed data. *Remote Sens. Environ.* **10**(2), 135–163 (1980)
21. Gevana, D., Camacho, L., Carandang, A., Camacho, S., Im, S.: Land use characterization and change detection of a small mangrove area in Banacon Island, Bohol, Philippines using a maximum likelihood classification method. *Forest Sci. Technol.* **11**(4), 197–205 (2015)

22. Lewis, H., Brown, M.: A generalized confusion matrix for assessing area estimates from remotely sensed data. *Int. J. Remote Sens.* **22**(16), 3223–3235 (2001)
23. Visa, S., Ramsay, B., Ralescu, A.L., Van Der Knaap, E.: Confusion matrix-based feature selection. *MAICS*. **710**, 120–127 (2011)
24. Payne, C., Panda, S., Prakash, A.: Remote sensing of river erosion on the Colville River, North Slope Alaska. *Remote Sens. (Basel)*. **10**(3), 397 (2018)
25. Yue, H., Li, Y., Qian, J., Lin, Y.: A new accuracy evaluation method for water body extraction. *Int. J. Remote Sens.* **41**(19), 1–32 (2020)
26. Kinnura, M., M. Higo, K. Lorsirirat, and S. Kumlungkeng, Identifying significant tributaries from human impacted sedimentary system. (2002).
27. Morisawa, M.: Distribution of stream-flow direction in drainage patterns. *J. Geol.* **71**(4), 528–529 (1963)